J|A|C|S
COMMUNICATIONS

Published on Web 01/16/2004

In *Rhodobacter sphaeroides* Respiratory Nitrate Reductase, the Kinetics of Substrate Binding Favors Intramolecular Electron Transfer

Bettina Frangioni,[†] Pascal Arnoux,[‡] Monique Sabaty,[‡] David Pignol,[‡] Patrick Bertrand,[†] Bruno Guigliarelli,[†] and Christophe Léger*,[†]

Laboratoire de Bioénergétique et Ingénierie des Protéines, CNRS, 31 chemin J. Aiguier, 13402 Marseille, France, and CEA/Cadarache, DSV, DEVM, Laboratoire de Bioénergétique Cellulaire, 13108 St Paul les Durance Cedex, France

Received September 9, 2003; E-mail: christophe.leger@ibsm.cnrs-mrs.fr

The respiratory nitrate reductase (NapAB) from *Rhodobacter sphaeroides*[1] is a 108 kDa, periplasmic, heterodimeric enzyme which belongs to the DMSO reductase family[2] and houses a molybdenum bis-MGD cofactor, a [4Fe-4S] cluster in close proximity to the active site, and two surface-exposed, *c*-type hemes. Here, we report a study of NapAB by protein film voltammetry[3] (PFV), and we present the first quantitative interpretation of the complex redox-state dependence of activity that has also been observed with several other related enzymes.[4] These results show that reduction potentials cannot always be directly used to understand the behavior of an enzymatic system under turnover conditions.

In PFV, a redox enzyme is adsorbed onto an electrode surface, in such a way that electron transfer (ET) is direct and fast. The redox state of the enzyme can be tuned by poising the electrode potential while the activity is measured as a current which is proportional to turnover number.[3] In the simplest cases,[5] the catalytic wave is sigmoidal and centered on the active-site reduction potential. In contrast, Figure 1 shows steady-state voltammograms for nitrate reduction by NapAB adsorbed onto a pyrolytic graphite edge (PGE) electrode.[6] As the electrode potential (E) is taken to more negative values, the activity first increases to a maximum (the current i decreases to a minimum), before it levels off at high driving force. This is remarkably counterintuitive, as activity decreases when E becomes lower than the reduction potential of the $Mo^{V/IV}$ couple[1] (-225 ± 10 mV), whereas the activity is expected to appear when E is sufficiently low that the catalytically competent Mo^{IV} state accumulates.

The qualitative interpretation of such waveshapes[3,4] is usually based on a mechanism such as that depicted in Scheme 1, which will now be used to model the data. Binding of substrate can occur to the Mo in its oxidation state V or IV, with dissociation constants $K_V = k_{-V}/k_V$ and $K_{IV} = k_{-IV}/k_{IV}$, respectively. The active site has to be fully reduced and bound to nitrate before the catalytic cycle is completed by formation and release of nitrite with a first-order rate constant k_c. We note $E^0_{V/IV}$ and $E^0_{V/IV,sat} = E^0_{V/IV} + (RT/F)\ln(K_V/K_{IV})$, the reduction potentials of the $Mo^{V/IV}$ couple in the absence of substrate and under saturating conditions, respectively.[7] The $Mo^{VI/V}$ transition of the nitrate-free form of the active site is not explicitly considered because the corresponding reduction potential is so high[1] that Mo^{VI} never accumulates in the electrode potential range over which catalysis is observed. The fact that no typical feature revealing sluggish interfacial ET[8] appears in the voltammograms suggests that redox equilibria are not displaced by turnover. Noting $e_X = \exp[(F/RT)(E - E^0_X)]$, the steady-state current equation for Scheme 1 reads[7] (see Supporting Information):

$$-2FA\Gamma k_c/i = 1 + e_{V/IV,sat} + (k_c/k_{IV}S)[(1 + e_{V/IV})/(1 + (k_V/k_{IV})e_{V/IV})] \quad (1)$$

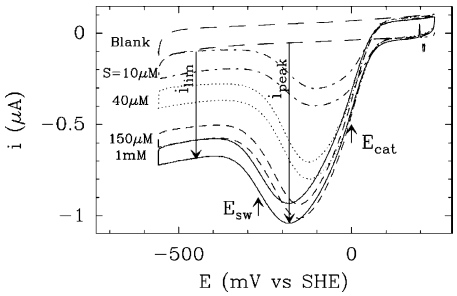

Figure 1. Catalytic voltammograms obtained for NapAB adsorbed at a PGE electrode. $T = 20$ °C, pH 7, electrode rotation rate $\omega = 4$ krpm, scan rate $\nu = 20$ mV/s. The voltammogram recorded in the absence of enzyme is plotted using long dashes. E_{cat} and E_{sw} are the inflection points of the wave, and S is the substrate (nitrate) concentration.

Scheme 1. Catalytic Cycle for the Reduction of Nitrate by NapAB[a]

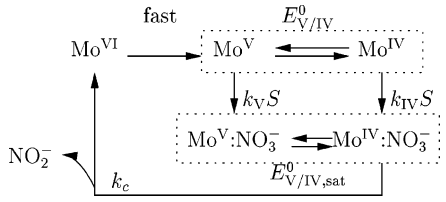

[a] Species within dotted boxes remain at equilibrium.

Provided that binding of substrate partly limits turnover, and is faster and weaker when the Mo ion is in the V oxidation state than when it is fully reduced ($k_V > k_{IV}$, $K_V > K_{IV}$), activity is the greatest at moderate driving force, when the reaction proceeds via Mo^V:NO_3^-. The values of E_{cat} and E_{sw} (Figure 1) can be derived from eq 1:

$$E_{cat} = E^0_{V/IV,sat} + (RT/F)\ln(1 + k_c/k_V S) \quad (2a)$$

$$E_{sw} = E^0_{V/IV} + (RT/F)\ln[(k_c + k_{IV}S)/(k_c + k_V S)] \quad (2b)$$

that is, activity appears at E close to $E^0_{V/IV,sat}$, while E_{sw} tends to $E^0_{V/IV}$ at low substrate concentration. From eq 1, it can also be shown that the limiting and peak currents depend on substrate concentration according to the Michaelis−Menten equation with Michaelis constants $K_m = k_c/k_{IV}$ and k_c/k_V, respectively.

The X-intercepts and average slope of the Hanes plots in Figure 2A gave $K_m = 30 \pm 5$ μM, $k_c/k_V = 7.5$ μM (thus $k_V/k_{IV} = 4.1$), and $2FA\Gamma k_c = 119 \pm 5$ nA. Using these values, all five

[†] CNRS.
[‡] CEA/Cadarache.

10.1021/ja0384072 CCC: $27.50

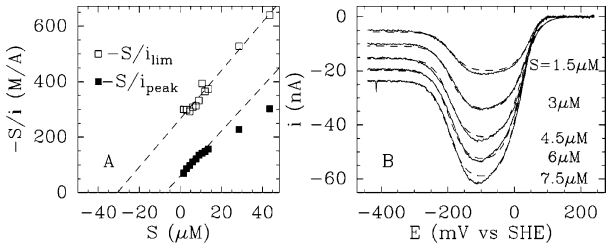

Figure 2. Panel A: Hanes plots of S/i_{lim} (□) and S/i_{peak} (■) against S. Panel B: Best fit to eq 1 (dashed lines) of a set of catalytic voltammograms (plain lines). $T = 20$ °C, pH 7.8, $\omega = 6$ krpm, $\nu = 10$ mV/s. The data have been corrected by subtracting the voltammogram recorded before nitrate was added in the cell.

voltammograms in Figure 2B could be simultaneously fit to eq 1 with $E^0_{V/IV} = -185 \pm 5$ mV (in fair agreement with the value determined in ref 1, -225 ± 10 mV) and $E^0_{V/IV,sat} = -5 \pm 5$ mV.

In all cases but one,[9] multicentered Mo enzymes of the DMSO reductase family for which PFV data are available[3,4] (*E. coli* DMSO reductase, *Paracoccus pantotrophus* nitrate reductase, *E. coli* nitrate reductase, and *Synechococcus sp.* nitrate reductase) exhibit an optimal potential window for catalysis, as observed here for NapAB, and the waveshape is highly dependent on substrate concentration and/or pH. Moreover, except in the case of *E. coli* NarGHI,[10] (i) activity appears at low driving force, 100−200 mV above $E^0_{V/IV}$ (as predicted by eq 2a provided $K_V > K_{IV}$), and (ii) the "swich off" is observed at an electrode potential close (within 40 mV) to the reduction potential of the $Mo^{V/IV}$ couple (cf. eq 2b) (see Table S1).

Remarkably, eq 2a predicts that catalytic activity appears at E close to the reduction potential of the nitrate-saturated $Mo^{V/IV}$ couple even under nonsaturating conditions ($S \ll K_m$ in Figure 2B). This results directly from substrate binding being essentially irreversible in Scheme 1:[11] if substrate binding and release steps were at equilibrium, the catalytic waveshape would be sigmoidal with a substrate-concentration dependent midpoint potential given by:[5]

$$E_{cat} = E^0_{V/IV} + (RT/F)\ln[(1 + S/K_{IV})/(1 + S/K_V)] \quad (3)$$

thus E_{cat} would tend to $E^0_{V/IV}$ at low substrate concentration. While catalytic systems are maintained out of equilibrium during turnover, there are cases[5a] where the ratios of steady-state concentrations of intermediates are so close to their equilibrium values that the cycle can be understood on the basis of reduction potentials obtained from potentiometric (equilibrium) titrations. In contrast, the enzymes discussed here exemplify the situation where the presence of irreversible steps has a profound effect on the catalytic cycle.

In the case of NapAB, the fact that binding steps are not at equilibrium results in a large (ca. 200 mV) decrease in the driving force required to reduce the Mo^V ion and to produce nitrite. This has interesting consequences regarding intramolecular electron transfer. Indeed, the fact that the reduction potential of the proximal [4Fe-4S] cluster that donates electrons to the Mo active site (in NapAB) is substantially higher than that of the $Mo^{V/IV}$ couple (−80 versus −225 mV) seems to make the last intramolecular ET step endergonic. Although one may argue that it could yet be fast because of the small distance between the proximal cluster and the active site,[12] the present study sheds new light on the thermodynamic properties of this ET step: the reduction potential of the [4Fe-4S] cluster is sufficiently low that reduction of substrate-bound Mo^V by $[4Fe\text{-}4S]^+$ is exergonic, and the reduction potential of the substrate-free $Mo^{V/IV}$ couple is irrelevant.

Because the corresponding potentiometric data are not available in the case of most enzymes discussed here,[13] it is not yet possible to establish whether the mechanism we propose to explain favorable ET between the proximal [4Fe-4S] cluster and the Mo ion in NapAB applies to other multicentered enzymes of the DMSO reductase family.

The model presented here allows the very quantitative interpretation of the voltammetric data in the low, physiological substrate-concentration range ($S \le k_c/k_V = 7.5\ \mu M = K_m/4$): at a higher concentration of nitrate, the waveshape deviates from that predicted by eq 1, and the plot of S/i_{peak} against S in Figure 2A shows significant curvature. This occurs because as the rate of binding increases, other chemical steps become partly rate limiting and influence the waveshape. Work is in progress to determine which mechanism (more complex and general than that depicted in Scheme 1) is required to interpret the results over the entire range of substrate concentration.

Supporting Information Available: Table S1 and derivation of all equations (PDF). This material is available free of charge via the Internet at http://pubs.acs.org.

References

(1) Arnoux, P.; Sabaty, M.; Frangioni, B.; Guigliarelli, B.; Alric, J.; Adriano, J.-M.; Pignol, D. *Nat. Struct. Biol.* **2003**, *10*, 928−934.
(2) Hille, R. *Trends Biochem. Sci.* **2002**, *27*, 360−367.
(3) Léger, C.; Elliott, S. J.; Hoke, K. R.; Jeuken, L. J. C.; Jones, A. K.; Armstrong, F. A. *Biochemistry* **2003**, *42*, 8653−8662.
(4) (a) Heffron, K.; Léger, C.; Rothery, R. A.; Weiner, J. H.; Armstrong, F. A. *Biochemistry* **2001**, *40*, 3117−3126. (b) Anderson, L. J.; Richardson, D. J.; Butt, J. N. *Biochemistry* **2001**, *40*, 11294−11307. (c) Elliott, S. J.; Léger, C.; Pershad, H. R.; Hirst, J.; Heffron, K.; Ginet, N.; Blasco, F.; Rothery, R. A.; Weiner, J. H.; Armstrong, F. A. *Biochim. Biophys. Acta* **2002**, *1555*, 54−59. (d) Butt, J. N.; Anderson, L. J.; Rubio, L. M.; Richardson, D. J.; Flores, E.; Herrero, A. *Bioelectrochemistry* **2002**, *56*, 17−18.
(5) (a) Léger, C.; Heffron, K.; Pershad, H. R.; Maklashina, E.; Luna-Chavez, C.; Cecchini, G.; Ackrell, B. A. C.; Armstrong, F. A. *Biochemistry* **2001**, *40*, 11234−11245. (b) Léger, C.; Jones, A. K.; Roseboom, W.; Albracht, S. P. J.; Armstrong, F. A. *Biochemistry* **2002**, *41*, 15736−15746.
(6) Samples of NapAB were prepared as described in ref 1. The protein films were formed by painting a freshly polished PGE rotating electrode ($A = 0.3$ cm^2) with 1 μL of 90 μM NapAB solution. Experiments were performed under a nitrogen atmosphere, with buffers consisting of either 5 mM in each of CHES, HEPES, MES, TAPS, NaAc and 0.1 M NaCl (Figure 1), or 50 mM TRIS and 0.1 M NaCl (Figure 2).
(7) Notations: F, Faraday constant; R, gas constant; T, temperature; S, substrate concentration; A, electrode surface; Γ, electroactive coverage. The other symbols are defined in the text.
(8) Léger, C.; Jones, A. K.; Albracht, S. P. J.; Armstrong, F. A. *J. Phys. Chem. B* **2002**, *106*, 13058−13063.
(9) The only exception so far is *Alcaligenes faecalis* arsenite oxidase (Ellis, P. J.; Conrads, T.; Hille, R.; Kuhn, P. *Structure* **2001**, *9*, 125−132) which exhibits a sigmoidal waveshape (Hoke, K. R., Cobb, N., Hille, R., Armstrong, F. A., private communication). An EPR signal for the Mo^V has not been observed for this enzyme, and, accordingly, noncatalytic PFV data suggest that ET to the Mo is cooperative:[3] the instability of the Mo^V ion naturally explains that no extrema in the activity should appear. Sulfite oxidases, which are not members of the DMSO reductase family, do not show complex electrochemical modulation of catalytic activity (Elliott, S. J.; McElhaney, A. E.; Feng, C.; Enemark, J. H.; Armstrong, F. A. *J. Am. Chem. Soc.* **2002**, *124*, 11612−11613. Aguey-Zinsou, K.-F.; Bernhardt, P. V.; Kappler, U.; McEwan, A. G. *J. Am. Chem. Soc.* **2003**, *125*, 530−535).
(10) *E. coli* nitrate reductase exhibits extremely complex waveshapes (Figure 2 in ref 4c), which cannot be explained by the simple considerations presented here.
(11) In model compounds relevant to the DMSO reductase family, reduction of oxide proceeds according to second order, irreversible kinetics, and the large, negative entropy of activation indicates an associative transition state involving considerable Mo−O(substrate) bond making (Lim, B. S.; Holm, R. H. *J. Am. Chem. Soc.* **2001**, *123*, 1920−1930), in accordance with density functional calculations (Webster, C. E.; Hall, M. B. *J. Am. Chem. Soc.* **2001**, *123*, 5820−5821). In *Rb. capsulatus* DMSO reductase, formation of the enzyme−substrate complex (as opposed to the subsequent, first-order catalytic step) is rate determining at low pH (Adams, B.; Smith, A. T.; Bailey, S.; McEwan, A. G.; Bray, R. C. *Biochemistry* **1999**, *38*, 8501−8511).
(12) Page, C. C.; Moser, C. C.; Chen, X.; Dutton, P. L. *Nature* **1999**, *402*, 47−52.
(13) The recently determined crystal structure of *E. coli* nitrate reductase revealed that a proximal [4Fe-4S] in NarG has previously escaped characterization (Bertero, M. G.; Rothery, A. R.; Palak, M.; Hou, C.; Lim, C.; Lim, D.; Blasco, F.; Weiner, J. H.; Strynadka, N. C. J. *Nat. Struct. Biol.* **2003**, *10*, 681−687). In *E. coli* DMSO reductase, an equivalent, yet unidentified, cluster may be present in DmsA (Rothery, R. A., private communication).

JA0384072